Published for SISSA by Springer

Received: *August 20, 2023*
Revised: *October 12, 2023*
Accepted: *October 18, 2023*
Published: *October 31, 2023*

JHEP10(2023)189

# Circular string in a black p-brane leading to chaos

**Pinaki Dutta, Kamal L. Panigrahi and Balbeer Singh**

*Department of Physics, Indian Institute of Technology Kharagpur, Kharagpur 721 302, India*

*E-mail:* coolguddu0815@kgpian.iitkgp.ac.in, panigrahi@phy.iitkgp.ac.in, curiosity1729@kgpian.iitkgp.ac.in

Abstract: We consider a pulsating string near a non-extremal black p-brane (p=5 and p=6) and investigate the chaos in the corresponding string dynamics by examining the Fast Lyapunov indicator(FLI) and Poincare section. In our system, the energy and the charge play the role of control parameters. For generic values of these parameters, the numerical results show that the dynamics primarily fall into three modes: capture, escape to infinity, and quasiperiodic depending on the initial location (near to or far away from the black brane horizon) of the string. Finally, probing for different values of the winding number ($n$) the dynamics turns out to be sensitive to $n$. In particular, we observe the point particle ($n = 0$) scenario to be integrable whereas at higher $n$ the dynamics seems to be chaotic.

Keywords: Black Holes in String Theory, Bosonic Strings, P-Branes, Integrable Field Theories

ArXiv ePrint: 2307.12350



https://doi.org/10.1007/JHEP10(2023)189

## Contents



JHEP10(2023)189

## 1 Introduction

The investigation of chaotic systems has captivated numerous prominent researchers across different fields for several decades. Defining chaos rigorously remains a subject of ambiguity to this day. However, it is now widely accepted that the sensitivity to the initial condition of a classical dynamical system subject to some constraints is believed to define a chaotic system. Here, we will also follow this definition accompanied by well-known chaotic indicators such as the Poincare section, Fast Lyapunov indicator(FLI), etc.

In a true sense, integrability means that a system of differential equations can be solved by a method of quadratures i.e. its solution can be obtained in a finite number of algebraic operations [1]. Most of the studies involve the existence of the integrals of motion for showing the integrability of a dynamical system. Due to the Liouville theorem, a Hamiltonian system of N degrees of freedom is said to be integrable if it has exactly N integrals of motion and these conserved quantities $Q_i = f(p, q)$ including the energy can be used to construct the solution where the corresponding phase space is 2N dimensional consisting of coordinates $q_i$ and the canonical momenta $p_i$. These charges define a N-dimensional torus in the phase space. To every tori of rational winding number, there exists infinitesimally close to it, the tori having irrational winding number. Such a tori is known as KAM tori. According to the KAM theorem, when deformed the majority of the tori undergo a slight deformation but manage to survive. However, tori characterized by the rational frequency ratios experience destruction and therefore leading to chaotic motion on these tori. For such a system, integrability and chaos are considered to be complementary to each other.

The dynamical behavior of a point particle in various curved backgrounds has been extensively studied [2–9]. Around a black hole spacetime, the dynamics turn out to be integrable [2]. However, the dynamics of such a geodesic becomes chaotic and non-integrable

if we consider more complicated geometries like in [8–10]. Moreover, the point particle dynamics near the horizon shows chaotic behaviour [11–13]. Even after all these developments geodesics are not considered as the most suitable means for investigating the chaos produced by black holes. Despite the fact that geodesics being integrable in a large class of simple backgrounds, they exhibit thermalisation and chaos due to finite Hawking temperature. This motivates to work with the string dynamics. The works of Hadamard-Anosov and others [14–19] delving into the constant curvature spaces, have shed light on the sensitive instability of phase space trajectories within them- a characteristic feature of chaos. It appears that chaos is a recurring feature in the dynamics of semiclassical strings within AdS backgrounds [14, 19–21] with the notable exceptions for e.g, $AdS_5 \times S^5$ in which string dynamics turns out to be integrable, see [22–25]. All these advancements [15, 21, 26–34] collectively indicate that the class of string integrable backgrounds constitutes only a limited subset within the larger class of particle integrable backgrounds. The (non)-integrability aspect can also be considered when examining the behavior of string dynamics in Dp-branes [35, 36]. Previous studies [35] have shown that the classically extended string in Dp-brane in extremal scenarios having charge as the interpolation parameter between flat space and $AdS_5 \times S^5$ are non-integrable. In this paper, our aim is to explore this concept and conduct a numerical analysis of the circular string dynamics in a black p-brane. Specifically, we will focus on two cases: p=5 and p=6. We shall begin with the non-extremal scenarios first and then eventually examine the extremal situation as well by means of varying the suitable parameter.

Another interesting paradigm in recent times is the remarkable application of quantum information theoretic tools to study the quantum effects of gravity. Black holes are not only quantum in nature but also thermal and therefore share the basic property of chaos which in the light of quantum information are commonly postulated to be the fastest scramblers in Nature [37]. For a finite temperature QFT, it is well-known that the defining characteristic of chaos is bounded by what is called Maldacena, Shenker, Standford (MSS) bound given as: $\lambda \leq 2\pi k_B T$ [38]. Currently, such a bound is saturated by holographic dual models such as SYK model [39–42]. The relationship between the chaos bound and the study of string dynamics in p-black branes has not been explored thus far. A generalized bound inequality for string dynamics in AdS geometries has been predicted in [43]. Our numerical investigation of the Lyapunov exponent associated with the orbits of the different string modes, to our surprise, suggests the existence of such a bound even though the bound was originally formulated for the field theories having classical gravity dual. Several efforts have been made to investigate the existence of such a bound in point particle dynamics [12, 44–49]. The rest of the paper is organized as follows. In section 3.1 and 3.2, we analyze the pulsating string in non-extremal charged and neutral p=5 brane respectively, using the underlying Hamiltonian dynamics. In the next subsection 3.3, we repeat a similar analysis for p=6 brane. In section 4, we discuss the role of the winding number pertaining to our study. Finally, in section 5, we summarize the numerical results of our analysis and give possible future directions.



JHEP10(2023)189

## 2 Black p-branes

In this section, we shall briefly explain the black p-branes in D=10 dimensions. Non-extremal black p-branes are the solutions of 10-dimensional low energy string theory [50, 51] and the corresponding metric ($p < 7$) is:

$$ds^2 = -\Delta_+ \Delta_-^{-1/2} dt^2 + \Delta_-^{1/2} \sum_{i=1}^{p} dx_i^2 + \Delta_+^{-1} \Delta_-^{\gamma} dr^2 + r^2 \Delta_-^{\gamma+1} d\Omega_{8-p} \tag{2.1}$$

where $\Delta_\pm = 1 - (\frac{r_\pm}{r})^{7-p}$, $\gamma = -\frac{1}{2} - \frac{5-p}{7-p}$ with $r_+$ and $r_-$ representing outer horizon and inner horizon radii respectively. The charge and mass per unit p-volume of the black brane are respectively given by

$$Q = \frac{7-p}{2}(r_+ r_-)^{(7-p)/2}$$
$$M = \frac{\Omega_{8-p}}{2k_{10}^2}\Big((8-p)r_+^{7-p} - r_-^{7-p}\Big)$$

where $\Omega_{8-p}$ is the volume of unit $(8-p)$- sphere and $k_{10}^2 = 8\pi G_{10}$.

Black-p-branes are characterized by a non-zero Hawking temperature which can be derived by a series of transformations [52–54] as given below:

$$r^{7-p} = \tilde{r}^{7-p} + r_-^{7-p}, \quad \tilde{r}_+^{7-p} = \mu^{7-p} \cosh^2\beta, \quad \tilde{r}_-^{7-p} = \mu^{7-p} \sinh^2\beta$$

This reduces the metric (2.1) to the form:

$$ds^2 = H^{-1/2}\Big(-f dt^2 + \sum_{i=1}^{p} dx_i^2\Big) + H^{1/2}\Big(f^{-1}dr^2 + r^2 d\Omega_{8-p}\Big) \tag{2.2}$$

where $H = 1 + (\frac{r_-}{r})^{7-p}$ and $f = 1 - (\frac{\mu}{r})^{7-p}$

Then we need to expand the metric in the vicinity of horizon, followed by a Wick rotation of the time coordinate. The periodicity of the Euclidean time gives the inverse temperature [53, 54]

$$\beta = \frac{4\pi\mu\cosh\beta}{7-p}$$
$$or \quad \beta = 2\pi\left(\frac{2r_+}{7-p}\left[1 - \left(\frac{r_-}{r_+}\right)^{7-p}\right]^{\frac{-5+p}{2(7-p)}}\right)$$

When $r_- = 0$, we have the neutral black brane solution:

$$ds^2 = -\left(1 - \left(\frac{r_0}{r}\right)^{7-p}\right)dt^2 + \left(1 - \left(\frac{r_0}{r}\right)^{7-p}\right)^{-1} dr^2 + r^2 d\Omega_{8-p} + \sum_{i=1}^{p} dx_i^2 \tag{2.3}$$

One can also obtain the supersymmetric extremal black brane solutions by setting $r_+ = r_-$ and then performing a change of coordinate $\tilde{r}^{7-p} = r^{7-p} - r_+^{7-p}$, we find

$$ds^2 = \left(1 + \left(\frac{r_0}{r}\right)^{7-p}\right)^{-1/2}\Big(-dt^2 + \sum_{i=1}^{p} dx_i^2\Big) + \left(1 + \left(\frac{r_0}{r}\right)^{7-p}\right)^{1/2}\Big(dr^2 + r^2 d\Omega_{8-p}\Big) \tag{2.4}$$



JHEP10(2023)189

The integrability of strings and geodesics in such extremal backgrounds have been studied through Normal Variational Equations (NVE) approach in [10, 35]. Note that such an approach can be implemented via metric (2.2). However our main objective is to study the behavior of closed string in p-branes through numerical analysis. To achieve this goal, we will pivot ourselves particularly around two types of branes namely p=5 and p=6. These branes offer more feasible access in handling the situation numerically that can be realized. However, when dealing with branes of lower dimensions, we have to deal with more coordinates transverse to the brane which need to be eliminated. Typically, this is achieved through a consistent truncation method [55, 56] but we shall completely ignore it and plan to address it in the future.

## 3 Circular string in p-brane

The propagation of a closed circular string in any arbitrary curved background can be modeled by the Polyakov action given as,

$$S = -\frac{1}{2\pi\alpha'}\int d\sigma d\tau \sqrt{-g} g^{\alpha\beta} G_{\mu\nu}(\partial_\alpha X^\mu \partial_\beta X^\nu) \tag{3.1}$$

where $\alpha' = l_s^2$ ($l_s$ represents the string length). $X^\mu$ represents the target space co-ordinates, $G_{\mu\nu}$ is the target space metric and $g_{\alpha\beta}$ is the worldsheet metric. We utilise the reparameterization and Weyl symmetries of the action and fix the conformal gauge, $g^{\alpha\beta} = \eta^{\alpha\beta}$. In this gauge, the vanishing of energy-momentum tensor $T_{\alpha\beta} = 0$ leads to the following constraints

$$G_{\mu\nu}\partial_\tau X^\mu \partial_\sigma X^\nu = 0 \tag{3.2}$$

$$G_{\mu\nu}\Big(\partial_\tau X^\mu \partial_\tau X^\nu + \partial_\sigma X^\mu \partial_\sigma X^\nu\Big) = 0 \tag{3.3}$$

The target space metric $G_{\mu\nu}$ is given by equation (2.1). Now, we use the pulsating string ansatz for p = 5 brane and the action (3.1), to construct the Hamiltonian and the corresponding equation of motion.

### 3.1 Black 5-brane

We will consider the following ansatz representing the circular string

$$t = t(\tau)\,, r = r(\tau)\,, \phi_1 = \phi_1(\tau)\,, \phi_2 = \phi_2(\tau)\,, \phi_3 = n\sigma \tag{3.4}$$

where $n$ denotes the winding number of the string along $\phi_3$ direction. We assume the spatial coordinates $x^i$ are constant.

In this case, $\mathrm{d}\Omega_3 = d\phi_1^2 + \sin^2\phi_1 d\phi_3^2 + \cos^2\phi_1 d\phi_2^2$. Substituting in the Polyakov action (3.1), we get the following Lagrangian

$$L = -\frac{1}{2\pi\alpha'}\Big(\Delta_+\Delta_-^{-1/2}\dot{t}^2 - \Delta_+^{-1}\Delta_-^{-1/2}\dot{r}^2 - r^2\Delta_-^{1/2}(\dot{\phi_1}^2 + \cos^2\phi_1\dot{\phi_2}^2) + \Delta_-^{1/2}r^2n^2\sin^2\phi_1\Big)$$

where $\Delta_\pm(r) = 1 - (\frac{r_\pm}{r})^2$ and dot represents the derivative with respect to $\tau$.



JHEP10(2023)189

The corresponding Hamiltonian and the equations of motion can be obtained as follows:

$$H = \frac{\pi\alpha'}{2}\left(\Delta_+\Delta_-^{1/2}p_r^2 + \frac{p_{\phi_1}^2}{r^2\Delta_-^{1/2}} + \frac{p_{\phi_2}^2}{r^2\Delta_-^{1/2}\cos^2\phi_1} - \frac{p_t^2}{\Delta_+^{-1}\Delta_-^{1/2}}\right) + \frac{1}{2\pi\alpha'}n^2r^2\Delta_-^{1/2}\sin^2\phi_1$$

$$\dot{p_t} = 0 \tag{3.5}$$

$$\dot{t} = -\pi\alpha'\Delta_+\frac{p_t}{\Delta_-^{1/2}} \tag{3.6}$$

$$\dot{p_r} = \frac{\pi\alpha'}{2}\frac{\partial}{\partial r}\left(p_t^2\Delta_-^{-1/2}\Delta_+ - p_r^2\Delta_-^{1/2}\Delta_+ - \left(p_{\phi_1^2} + \frac{p_{\phi_2^2}}{\cos^2\phi_1}\right)\frac{1}{r^2\Delta_-^{1/2}} - \frac{n^2}{2\pi\alpha'}r^2\Delta_-^{1/2}\sin^2\phi_1\right) \tag{3.7}$$

$$\dot{r} = \pi\alpha'\Delta_+\Delta_-^{1/2}p_r \tag{3.8}$$

$$\dot{p}_{\phi_1} = \frac{-\pi\alpha'}{r^2\phi_1}p_{\phi_2}^2\sec^2\phi_1\tan\phi_1 - \frac{n^2}{\pi\alpha'}r^2\Delta_-^{1/2}\sin\phi_1\cos\phi_1 \tag{3.9}$$

$$\dot{\phi_1} = \pi\alpha'\frac{p_{\phi_1}}{r^2} \tag{3.10}$$

$$\dot{p}_{\phi_2} = 0 \tag{3.11}$$

$$\dot{\phi_2} = \pi\alpha'\frac{p_{\phi_1}}{r^2\Delta_-^{1/2}\cos^2\phi_1} \tag{3.12}$$

Equations (3.5) and (3.11) give two constants of motion- $p_t$ = E (energy) and $p_{\phi_2}$ = l (angular momentum). The constraint (3.2) is trivially satisfied, however equation (3.3) gives H = 0.

### A. String trajectory for different values of charge

Without loss of generality, we set the following initial conditions and parameters- $p_r(0) = 0$, $\phi_1(0) = 0$, E = 7, l = 8 to numerically solve the equations of motion and we set $\pi\alpha' = 1$, $n = 1$, $G_{10} = c = 1$ throughout the rest of the paper. We fix the mass M = $3\pi/8$, then the charge and mass satisfy the inequality $Q \leq 4M/\pi$ for unit volume. Considering the charge Q as a control parameter, we monitor the string dynamics by varying Q. For the visualisation of string dynamics, we mostly follow the procedures of [57]. In figure 1, we present the string trajectory for two different initial radial positions of the string. First, we consider the string initially close to the brane (figure 1(a),(b)). For a small charge (Q = 0.1), we find that the string gets trapped in the black brane very quickly, whereas in the extremal limit (Q = 1.5) the string deviates from the horizon and rapidly escapes to infinity. However, when we keep the string at a large distance away from the brane (figure 1(c),(d)), the string escapes to infinity for both small and large value of charge. However, the rate of escape is very small unlike the first screnario (figure 1(b)).

### B. Fast Lyapunov indicator

One of the salient features of the chaotic system is that its dynamics are extremely sensitive to the initial condition for which one has to study the chaotic indicators. The Largest Lyapunov Exponent(LLE) is a commonly used method which is based on the algorithm of



JHEP10(2023)189

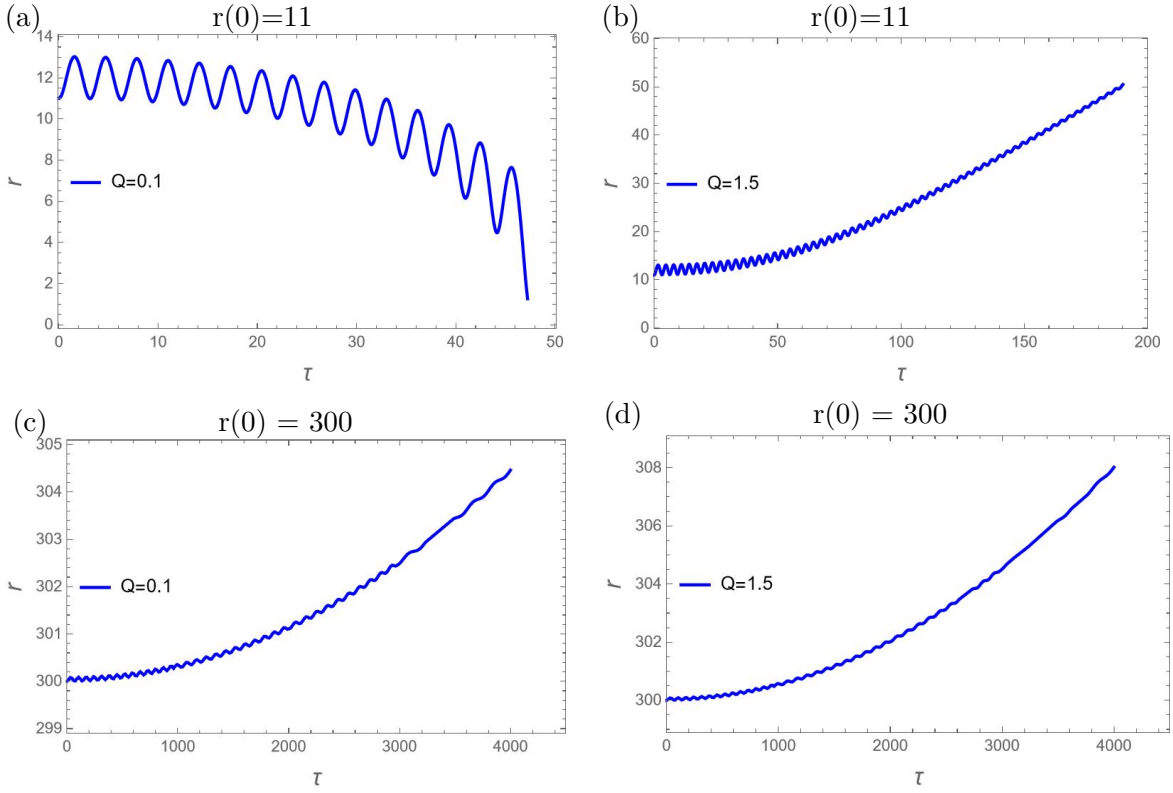


**Figure 1**. Plot showing the evolution of radial coordinate for different charges (Q=0.1,1.5) with different initial conditions r(0) = 11 (top panel) and r(0) = 300 (bottom panel).

measuring the average separation between the two initially nearby trajectories to characterize the nature (regular or chaotic) of orbits. However, there are some subtilities regarding LLE, for instance, sometimes it costs a large computation time to achieve a stable limiting value. Also, LLE is not suitable for distinguishing different regular orbits. Reference [58] shows that the value of LLE is not co-ordinate invariant and so not reliable for relativistic systems. Some of these issues can be overcome by implementing a closely related method known as Fast Lyapunov Indicator (FLI). FLI is quicker for detecting chaos and order and easier to implement. A detailed discussion on the Lyapunov indicators can be found in [59–61]. In this work, we mostly employ FLI [57, 59, 62] which is based on the following definition:

$$FLI = \log_{10} \frac{||\mathbf{d}(t)||}{||\mathbf{d}(0)||} = \lambda t \tag{3.13}$$

where $\lambda$ is the LLE, $\mathbf{d}(0)$ represents the initial separation between two nearby trajectories and $\mathbf{d}(t)$ represents the separation at time t. Thus from this equation, the FLI increases linearly (approximately) with $t$ for chaotic orbit with a positive slope whereas the slope is equal to zero for integrable motion. Note that, if the slope is very close to zero then orbit is quasi-periodic. In other words, the distance between two orbits increases exponentially for chaotic orbit and linearly (approximately) for non-chaotic orbit. For practical computation,



JHEP10(2023)189

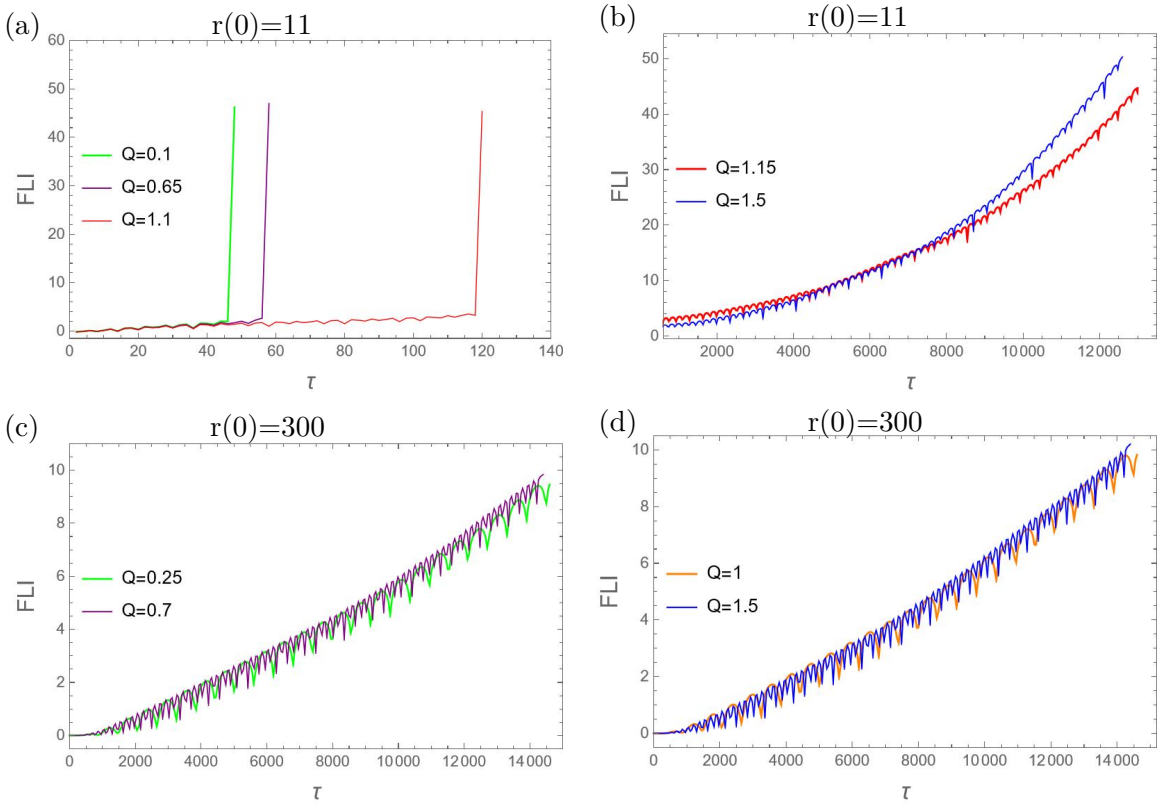


**Figure 2**. Plot showing the behaviour of FLI for different Q with different initial conditions r(0) = 11 (top panel) and r(0) = 300 (bottom panel).

we use the following expression:

$$FLI(t) = -k(1 + \log_{10}||d(0)||) + \log_{10}\frac{||d(t)||}{||d(0)||} \tag{3.14}$$

where $k(k = 0, 1, 2\ldots)$ denotes the number of renormalization. We choose $||d(0)|| \approx 10^{-7}$ and $||d(t)|| = 0.1$ as critical value to implement the process of renormalization. Now, in order to speculate the string dynamics, especially on the intermediate charges, we present FLIs in figure 2. When $r(0) = 11$ and Q = 0.1, 0.65, 1.1 (figure 2(a)), the FLI curve increases linearly at the beginning and then becomes vertical. The underlying reason for the sudden jump is due to the capture of the string in the black brane. Because of this collapse of string orbit, the calculation stopped at that instance and with the further increase of that critical times, we observe a shoot-up in FLI. Note that the time of capture increases with charge. However, when $Q > 1.1$ (figure 2(b)), the FLI increases approximately linearly and the string escapes to infinity. The rate of escape increases very slightly with charge as evident from the corresponding value of FLI. Next, we concentrate on $r(0) = 300$ (figure 2(c),(d)). Here, the corresponding FLI curve shows a linear growth and the string escapes to infinity with uniform rate for all values of charges. We clearly observe the consistencies between figure 1 and 2. Thus by tuning control parameter(charge), we can visualise different chaotic modes.



JHEP10(2023)189

### 3.2 Neutral black 5-brane

Now, we investigate the chaotic dynamics by setting Q = 0. Then the metric (2.3) reduces to the product of 5-dimensional Euclidean space and 5-dimensional Schwarzschild one:

$$ds^2 = -\left(1 - \left(\frac{r_0}{r}\right)^2\right)dt^2 + \left(1 - \left(\frac{r_0}{r}\right)^2\right)^{-1} dr^2 + r^2 d\Omega_3 + \sum_{i=1}^{5} dx_i^2$$

With the same ansatz as we assumed in the beginning, we find the Hamiltonian

$$H = \frac{\pi\alpha'}{2}\left(\Delta_+ p_r^2 + \frac{p_{\phi_1^2}}{r^2} + \frac{p_{\phi_2^2}}{r^2\cos^2\phi_1} - \frac{p_t^2}{\Delta_+}\right) + \frac{1}{2\pi\alpha'} n^2 r^2 \sin^2\phi_1 \tag{3.15}$$

The equations of motion are (3.5)–(3.12) with $\Delta_- = 1$. After solving the equations of motion, one obtains various possible modes of the string. Here, we present the two asymptotic modes of the string - escape to infinity and long times oscillations around the event horizon in figure 3. We comment on the chaotic behaviour by numerically evaluating the Poincare section and Fast Lyapunov Indicator.

#### A. String trajectory

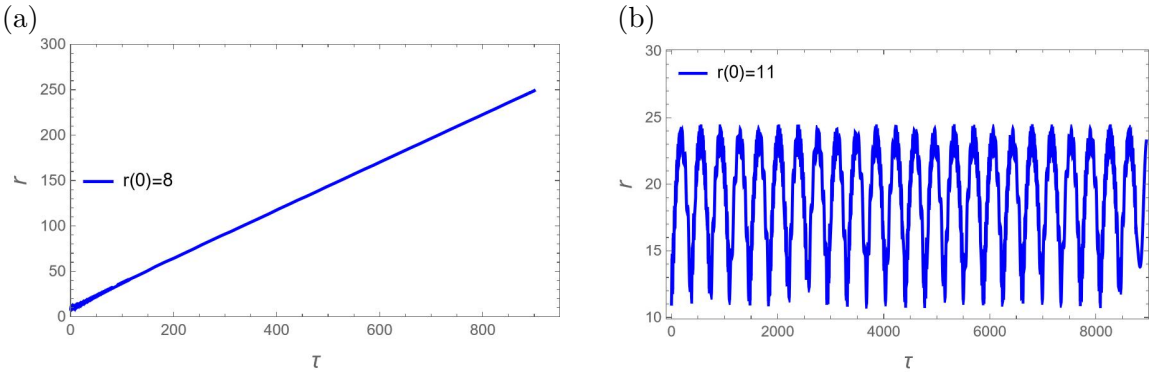


**Figure 3**. Plot showing the time evolution $r(\tau)$ indicating (a) escape to infinity and (b) quasiperiodic behavior of the string. For both the plots, we use E = 9, l = 8, n = 1, $r_+ = 1$. The initial conditions are $p_r(0) = 0$, $\phi_1(0) = 0$, r(0) = 8 for (a) and $p_r(0) = 0$, $\phi_1(0) = 0$, r(0) = 11 for (b).

#### B. Poincare section

Taking energy E as a control parameter, we provide the Poincare sections in the phase space (r, $p_r$) corresponding to different energies in figure 4. From the first two plots, we observe a quasi-periodic nature of the KAM tori when E = 10 and E = 12. However, the tori starts deforming with the further increase of energy ($E > 12$) and finally, when E = 15, we see a complete deformation and a collection of discrete points of the tori. Thus, with the increase of energy, our system becomes more and more chaotic.



JHEP10(2023)189

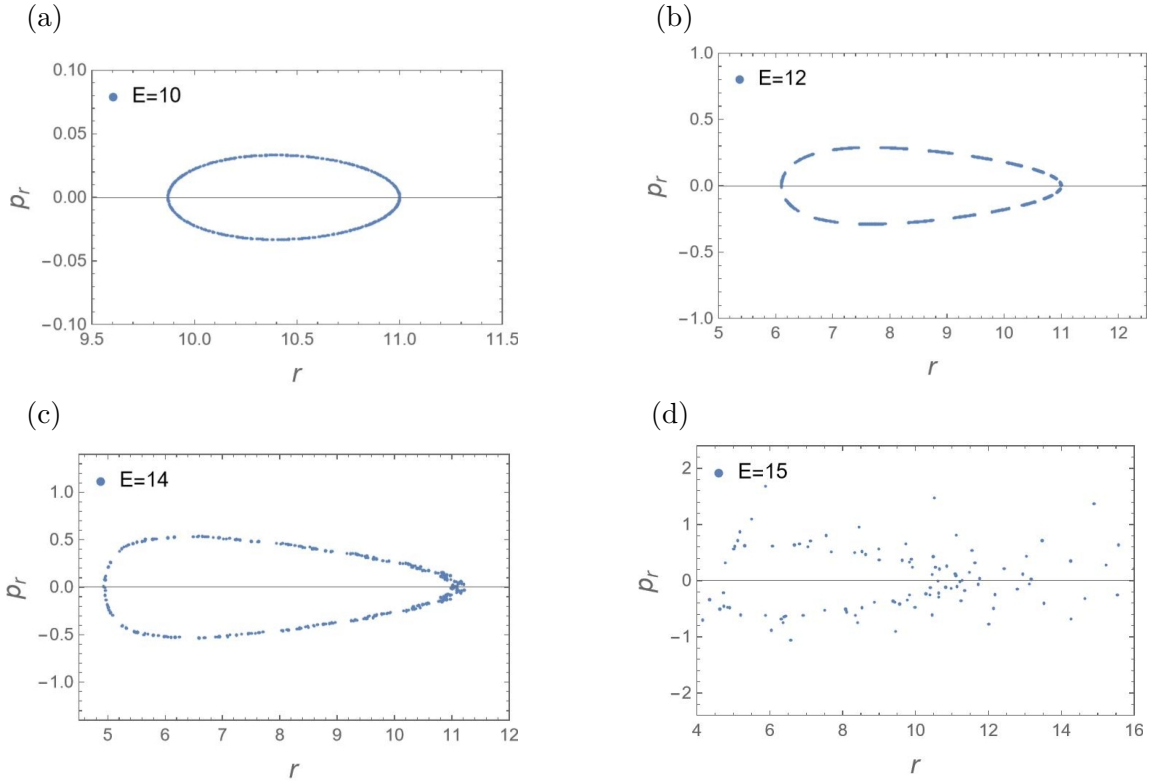


**Figure 4**. Plot showing the nature of poincare sections on the plane $\phi_1 = 0$ for (a) E = 10 (b) E = 12 (c) E = 14 (d) E = 15 indicating the distortion of tori with the increase of energy. We have set $r(0) = 11$, $p_r(0) = 0$, $\phi_1(0) = 0$, l = 8, n = 1, $r_+ = 1$.

### C. Fast Lyapunov indicator

We also present FLI in figure 5 for the corresponding energies. Note that for E=10 and E = 12, the corresponding string orbit is quasiperiodic (characterised by almost zero slope). However, with the increase of energy, the FLI increases almost linearly with a much higher slope. Thus, transition to chaos with the increase of E is consistent with figure 4.

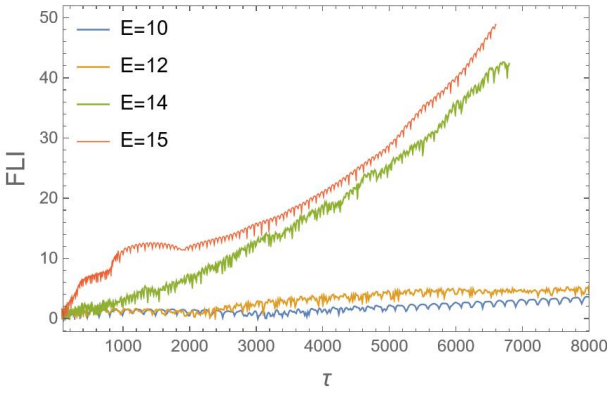


**Figure 5**. Plot showing the behaviour of FLI for $r(0) = 11$ in uncharged p=5 brane. The other parameters are same as that of figure 4.



JHEP10(2023)189

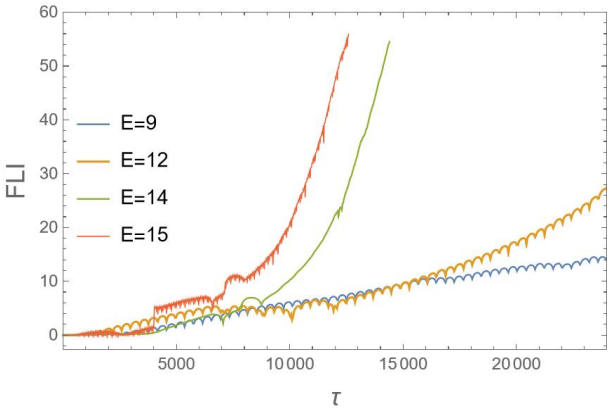


**Figure 6**. Plot showing the behaviour of FLI for $r(0) = 300$ in uncharged p=5 brane. The other parameters are same as that of figure 4.

As we increase the initial radial coordinate of the string (r(0)=300), we find a similar transition i.e the disappearance of the quasiperiodic behaviour and transition to more and more chaotic behaviour with the increase of energy (figure 6).

We now focus on the behaviour of pulsating string in p = 6 brane. In the next subsection, we construct our Hamiltonian and the equations of motion following the string ansatz and continue our discussion on chaotic dynamics.

### 3.3 Black 6-brane

We make the following ansatz for the circular string

$$t = t(\tau), \quad r = r(\tau), \quad \phi_1 = \phi_1(\tau), \quad \phi_2 = n\sigma$$

where $n$ represents the winding number of the string along $\phi_2$ direction.

In this case, $\mathrm{d}\Omega_3 = d\phi_1^2 + sin^2\phi_1 d\phi_2^2$. Substituting in the Polyakov action equation (3.2) we get the following Lagrangian

$$L = -\frac{1}{2\pi\alpha'}\left(\Delta_+\Delta_-^{-1/2}\dot{t}^2 - \Delta_+^{-1}\Delta_-^{1/2}\dot{r}^2 - r^2\Delta_-^{3/2}\dot{\phi_1}^2 + \Delta_-^{3/2}r^2n^2\sin^2\phi_1\right)$$

The corresponding Hamiltonian and the equation of motion are as follows:

$$H = \frac{\pi\alpha'}{2}\left(\Delta_+\Delta_-^{-1/2}p_r^2 + \frac{p_{\phi_1^2}}{r^2\Delta_-^{3/2}} - \frac{p_t^2}{\Delta_+\Delta_-^{-1/2}}\right) + \frac{1}{2\pi\alpha'}n^2\Delta_-^{3/2}r^2\sin^2\phi_1$$

$$\dot{p_t} = 0 \tag{3.16}$$

$$\dot{t} = -\pi\alpha'\Delta_-^{1/2}\Delta_+^{-1}p_t \tag{3.17}$$

$$\dot{p_r} = \frac{\pi\alpha'}{2}\frac{\partial}{\partial r}\left(-p_r^2\Delta_-^{-1/2}\Delta_+ + p_t^2\Delta_-^{1/2}\Delta_+^{-1} - p_{\phi_1^2}\frac{1}{r^2\Delta_-^{3/2}} - \frac{n^2}{2\pi\alpha'}r^2\Delta_-^{3/2}\sin^2\phi_1\right) \tag{3.18}$$

$$\dot{r} = \pi\alpha'\Delta_+\Delta_-^{-1/2}p_r \tag{3.19}$$

$$\dot{p}_{\phi_1} = -\frac{n^2}{\pi\alpha'}r^2\Delta_-^{3/2}\sin\phi_1\cos\phi_1 \tag{3.20}$$



JHEP10(2023)189

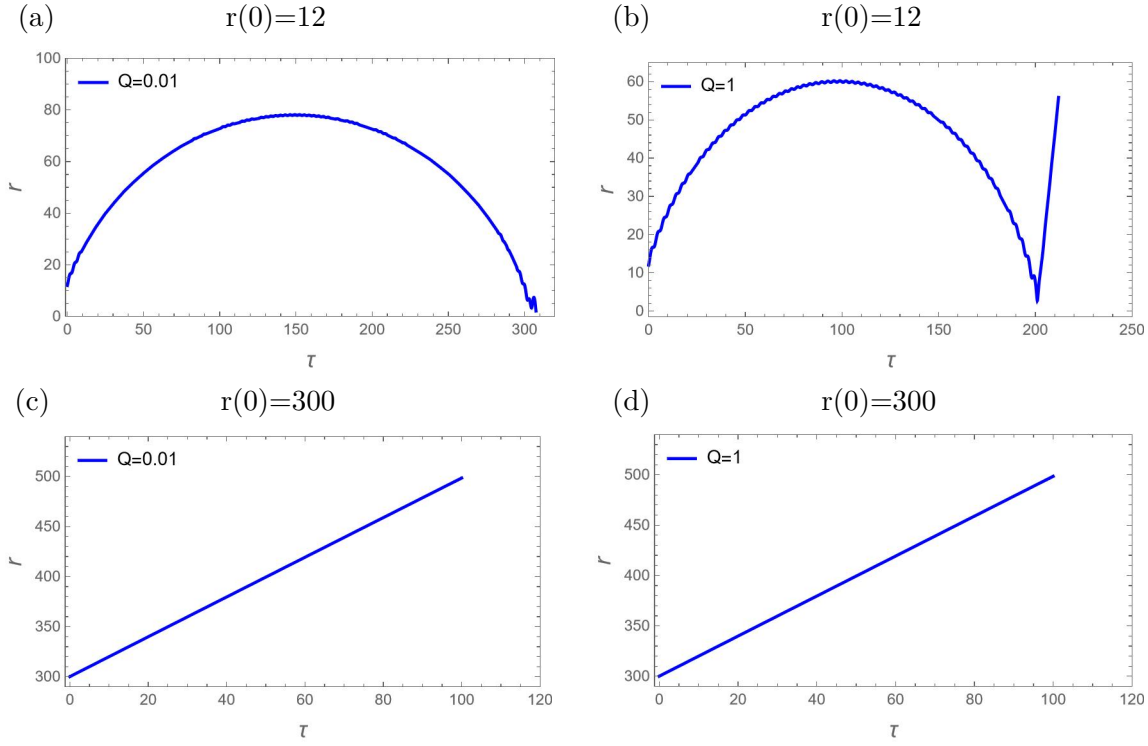


**Figure 7**. Plot showing the evolution of radial coordinate for different charges (Q=0.01,1) with different initial conditions r(0) = 12 (top panel) and r(0) = 300 (bottom panel).

$$\dot{\phi_1} = \pi\alpha' \frac{p_{\phi_1}}{r^2 \Delta_-^{3/2}} \tag{3.21}$$

The conformal gauge constraint gives H = 0 and the only constant of motion is the energy ($p_t = E$).

### A. String trajectory for different values of charge

Once again, we study the dynamics by increasing the charge Q for two different initial positions of the string. Without loss of generality, our choice of initial conditions and parameters are $p_r(0) = 2$, $\phi(0) = 0$, E = 7. We also set the mass M = 0.5, then the charge and mass satisfy the inequality $Q \leq 2M$. When we consider the string initially close to the brane, figure 7(a),(b) reflects the capture mode in the small charge limit and escape mode in the extremal limit. However, only the escape mode survives when the string is initially at a large distance away from the brane (figure 7(c),(d)). In the latter case, the overall dynamics is not much distinct from the corresponding p=5 case. To show this, we numerically evaluate FLI and display for different charges in figure 8.

### B. Fast Lyapunov indicator

First, we concentrate on the case when the string is initially close to the brane (figure 8(a),(b)). When $0 < Q < 0.5$, we observe that after some initial transient, the FLI curve becomes vertical indicating the capture of the string. However, unlike p = 5 case,



JHEP10(2023)189

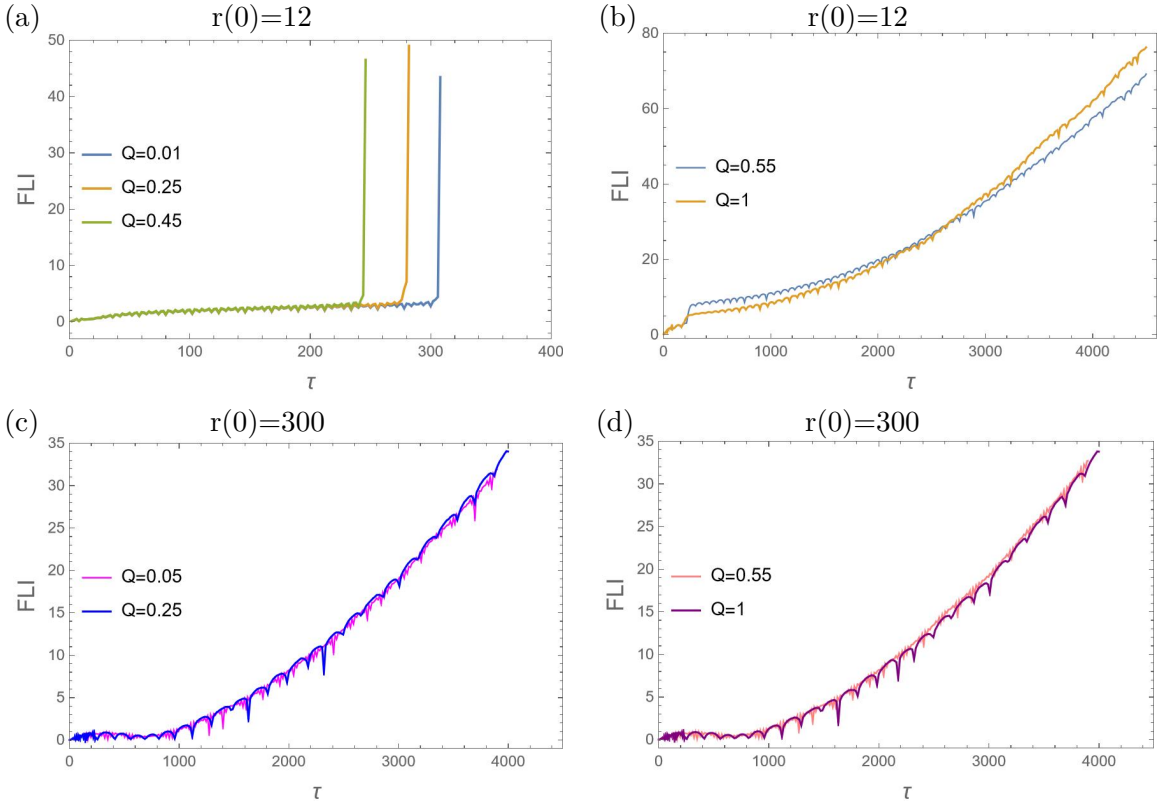


**Figure 8**. Plot showing the behaviour of FLI for different Q with different initial conditions r(0) = 12 (top panel) and r(0) = 300 (bottom panel).

the capture time decreases with charge. When $0.5 \leq Q \leq 1$, the string escapes to infinity. When the string is initially far from the brane, we find the string escapes to infinity with uniform rate (figure 8(c),(d)). The approximate linear growth of FLI curve reflects the chaotic motion.

Thus, in both charged p=5 and p=6 brane, the chaotic dyanmics do not change when the string starts from a large distance away from the brane!

Before concluding this section, we comment on the motion of closed string in uncharged p=6 brane. Note that when Q = 0, the corresponding metric becomes a product of 6-dimensional Euclidean space and 4-dimensional Schwarzschild. We obtain the following expression of Hamiltonian:

$$H = \frac{\pi\alpha'}{2}\left(\Delta_+ p_r^2 + \frac{p_{\phi_1}^2}{r^2} - \frac{p_t^2}{\Delta_+}\right) + \frac{1}{2\pi\alpha'} n^2 r^2 \sin^2\phi_1$$

The given system is equivalent to the motion of a string in four dimensional Schwarzschild space-time which has been studied in [16] where all the three asymptotic modes namely escape to infinity, capture of the string in the event horizon and escape to infinity via back scattering along with an infinite set of unstable periodic orbits has been reported. Therein a critical energy threshold has been figured out above which the system turns out to be chaotic.



JHEP10(2023)189

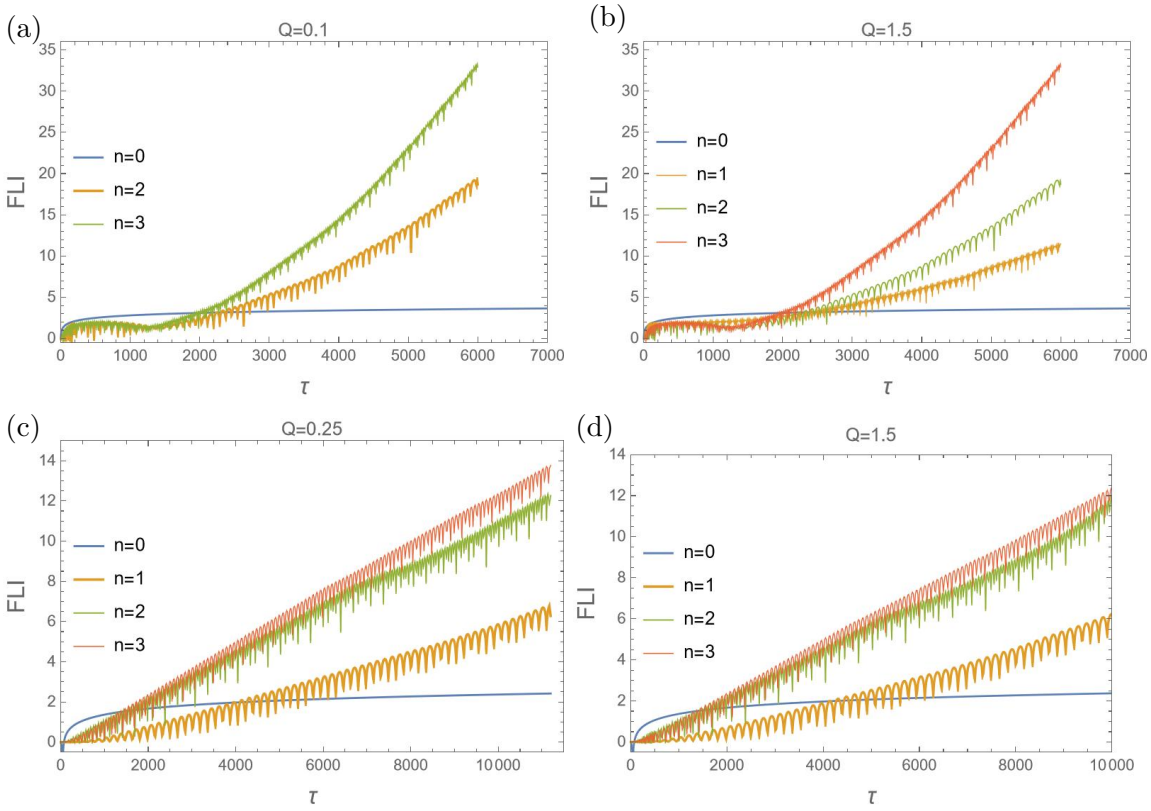


**Figure 9**. Plot showing the FLI for r(0) = 11 (top panel) and r(0) = 300 (bottom panel) for different $n$ and Q in charged p=5 brane. The other parameters are same as in figure 2.

## 4 Role of winding number

We shed some light on the role of winding number in string dynamics. The case $n$=0 corresponds to the point particle. The metric in equation (2.2) has (p+1) translational symmetries due to coordinates $x^\mu(\mu = 0, 1, \ldots, p)$ and so has (p+1) constants of motion. By suitable parametrization of the sphere in one higher dimensional sphere, it can be shown that the (D-p-2)-sphere possesses (D-p-2) constants of motion [35]. Therefore, in total, we have $p+1+D-p-2+1 = D$ integrals of motion where the additional integral of motion is coming from the Hamiltonian. Numerically, for $n$=0, the slope of FLI curve is equal to zero (see figure 9, 10, 11) which implies that the corresponding motion is integrable as expected. However, at higher winding numbers, the dynamics is essentially non-integrable which we explain below.

First, we consider the charged p=5 brane (figure 9). When $r(0) = 11$ (figure 9(a)) and Q = 0.1, the string escapes to infinity for $n > 1$. However, the string falls very quickly when $n = 1$ (see figure 2(a)). With increasing charge (upto Q = 1.5), we see the escape of the string for $n = 1$(figure 9(b)) also. When $r(0) = 300$ (figure 9(c),(d)), for both small and large value of Q, the string dynamics at higher $n$ is not very different from what we obtained for $n = 1$. Note that in all cases, FLI increases linearly and the rate of escape increases with n.



JHEP10(2023)189

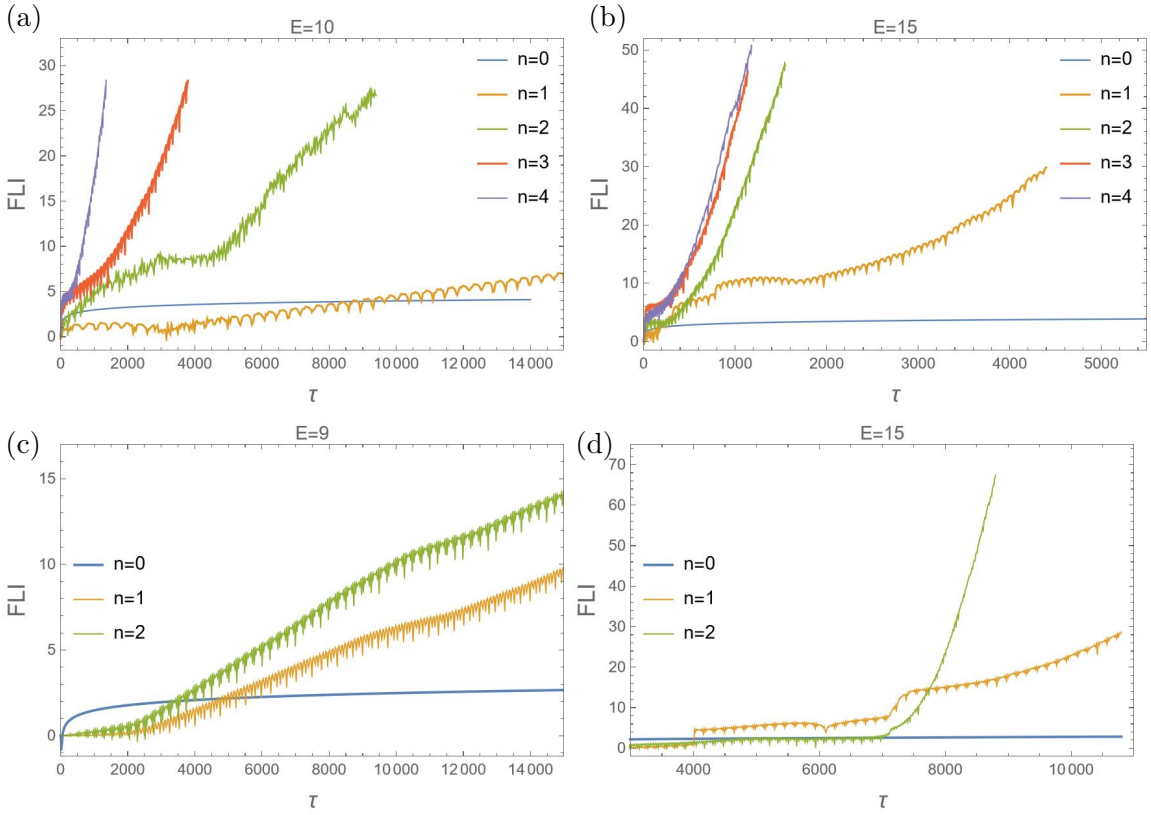


**Figure 10**. Plot showing the FLI for r(0) = 11 (top panel) and r(0) = 300 (bottom panel) for different $n$ and E in uncharged p=5 brane. The other parameters are same as in figure 5 and 6.

Next, we consider the uncharged p=5 brane (figure 10) where we have taken E as a control parameter. When $r(0) = 11$ (figure 10(a)) and E = 10, the FLI curve shows quasiperiodic motion for $n = 1$. The slope (approximately) increases with n reflecting the transition to chaos. For larger energy (E = 15) (figure 10(b)), we observe the escape mode for all $n \geq 1$. When $r(0) = 300$ (figure 10(c),(d)), the string escapes to infinity for both $n = 1$ and 2.

Thus, irrespective of where the string is initially located, the distance between two nearby trajectories increases with the winding number.

Now, we move on to charged p=6 brane (figure 11). First, we consider the case of $r(0) = 12$. For Q = 0.01, 0.45, 0.75 (figure 11(a),(b),(c)), the chaotic dynamics for $n = 1$ (see also figure 8(a)) and $n > 1$ are not much different except the fact that time of capture of the string decreases with $n$. At the extremal limit (Q = 1), the string escapes to infinity for all $n > 1$ (figure 11(d)), however, we do not observe any correlation between the rate of escape and $n$. When $r(0) = 300$ (figure 11(e),(f)), the string escapes to infinity for all charge and the rate of escape also increases with $n$.

Finally, we describe the role of $n$ and E in uncharged p=6 brane (figure 12) for two different initial locations r(0) = 12 and r(0) = 300. When r(0) = 12 and E = 4,6 we observe linear growth of FLI curve for $n \geq 1$ and the growth increases with n. By increasing energy (E = 10 and E = 11), we observe very quick capture for $n \geq 1$. Note that in the former, the



JHEP10(2023)189

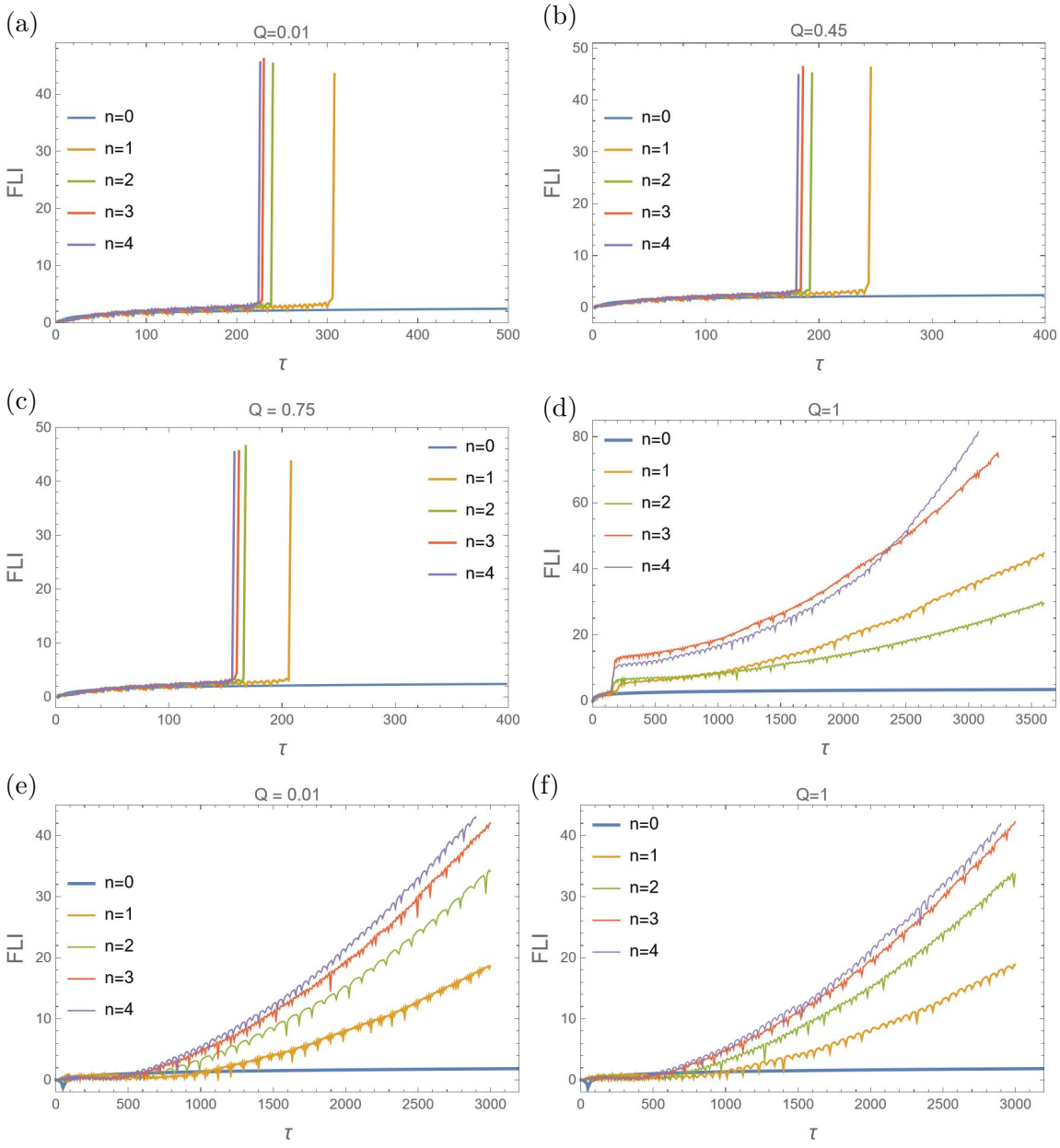


**Figure 11**. Plot showing the FLI for r(0) = 12 (top and middle panel) and r(0) = 300 (bottom panel) for different $n$ and Q in charged p=6 brane. The other parameters are same as in figure 8.

capture time is largest for n = 2 whereas in the latter, the capture time seems to decrease with n. However, for r(0) = 300 (figure 12(e),(f)), the string with any non-zero $n$ escapes to infinity for all E, the rate of escape increases with both $n$ and E.

## 5 Conclusion and future directions

In this work, we have numerically investigated the chaotic behaviour of a circular string in p=5 and p=6 brane and provide sufficient evidence of its chaotic motion. Based on the



JHEP10(2023)189

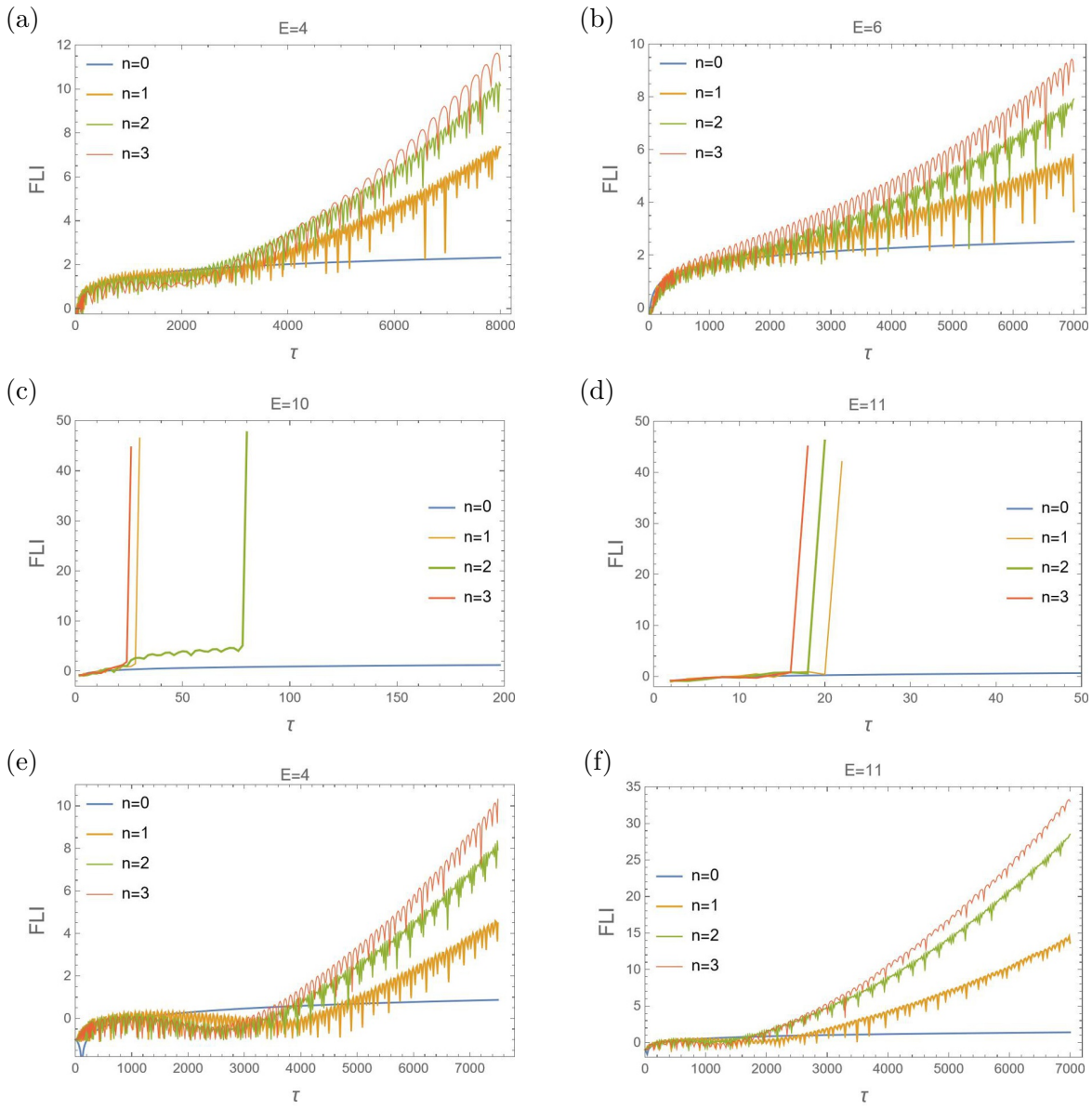


**Figure 12**. Plot showing the FLI for r(0) = 12 (top and middle panel) and r(0) = 300 (bottom panel) for different n and E in uncharged p=6 brane. The other parameters are same as in figure 11.

control parameters of our theory, we summarise the key findings as follows:

- Irrespective of the brane-background, the dynamics for $n = 0$ is integrable.
- In both charged p=5 and p=6 brane, when the string is initially at a large distance away from the brane, the charge seems to have an insignificant effect on the chaotic dynamics. The effect of winding number is only to increase the rate of escape of the string with $n$ for fixed charge!
- For the charged 5-brane, when the string initially starts near the brane, the capture time of the string increases as a function of charge and eventually at a large charge,



JHEP10(2023)189

the chaotic dynamics change from capture to escape mode. At a higher winding number, the string escapes to infinity, independent of charge and once again, the rate of escape increases with $n$.

- When we disable the charge (Q=0) in 5-brane and study the dynamics by suitably varying energy, independent of where the string is initially located, the dynamics change from quasi periodic to the escape mode at larger energies. However, the energy at which such a transition occurs that depends on the initial location. With the increase of $n$, the tendency of the string escaping to infinity increases.

- For both charged and uncharged 6-brane, when the string initially starts near the brane, our numerics show some non-monotonic behaviour of FLI curve with $n$ for a certain range of parameters.

- For the charged 6-brane, when $r(0) = 12$, we mostly observe the capture mode of the string, and the capture time decreases with the increase in both charge and $n$. Near the extremal limit, the dynamics change from capture to escape mode for all $n$.

- For the uncharged 6-brane and when r(0) = 12, we see a transition from escape to capture mode for $n \geq 1$ as we keep increasing control parameter(E). Going far away from the brane (r(0) = 300), we observe only the escape mode of the string. The dynamics at higher winding number follow the same trend, however, the linear growth of FLI seems to increase with $n$.

In future, we want to explore further the following thought-provoking questions:

- It was argued in [43] that for a closed circular string of winding number $n$ in an AdS black hole, the MSS bound generalizes to

$$\lambda \leq 2\pi k_B T n \tag{5.1}$$

For $n = 0$, the inequality (5.1) implies that $\lambda = 0$, which is consistent with our findings. We find strong evidence that the dynamics is sensitive to winding number. Also, note that $\beta \sim r_+$ for p=5 and $\beta \sim r_+\sqrt{1 - \frac{r_-}{r_+}}$ for p=6. This shows that with the increase of charge, Hawking temperature decreases for p=5 and increases for p=6. We do observe that the chaotic nature depends on charge/temperature at least when the string is initially close to the brane. This motivates us to do a comprehensive study of the near-horizon dynamics together with the relation (5.1) in the context of the p-black brane. We plan to address this gap by employing the NVE scheme [63, 64] in future work similar to [43].

- Expanding the directions of chaos, it would be interesting to study the scrambling properties of our system [65, 66].

- In the future for lower and higher dimensions of branes, we would like to do a detailed study of the generic p-branes involving a method of consistent truncation and dimensional reduction.



JHEP10(2023)189

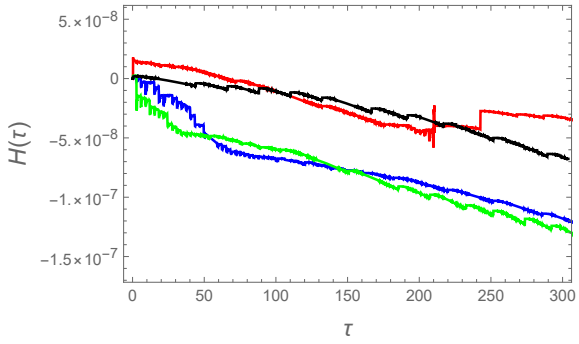


**Figure 13**. The evolution of H in charged p=5(blue), uncharged p=5(green), charged p=6(red) and uncharged p=6(black) brane.

- It would be interesting to explore the chaotic behaviour of string and point particle in intersecting non-extremal p-branes of [67].

**Numerical accuracy and error.** In this paper, we use the `Projection` method of `NDSolve` routine of `Mathematica` to solve the equations of motion. Note that we are dealing with nonlinear differential equations and one has to keep track of the constraint $H = 0$ at every integration step. We have checked this numerical accuracy and found that the maximum possible error (with in a reasonable computation time) is of the order of $10^{-6}$ (figure 13).

## Acknowledgments

The authors would also like to thank Manoranjan Samal for valuable comments on the manuscript.



## References

[1] V.P. Frolov, P. Krtous and D. Kubiznak, *Black holes, hidden symmetries, and complete integrability*, *Living Rev. Rel.* **20** (2017) 6 [arXiv:1705.05482] [INSPIRE].

[2] B. Carter, *Global structure of the Kerr family of gravitational fields*, *Phys. Rev.* **174** (1968) 1559 [INSPIRE].

[3] L. Bombelli and E. Calzetta, *Chaos around a black hole*, *Class. Quant. Grav.* **9** (1992) 2573 [INSPIRE].

[4] C.P. Dettmann, N.E. Frankel and N.J. Cornish, *Fractal basins and chaotic trajectories in multi-black hole space-times*, *Phys. Rev. D* **50** (1994) R618 [gr-qc/9402027] [INSPIRE].

[5] Y. Sota, S. Suzuki and K.-I. Maeda, *Chaos in static axisymmetric space-times. 1: vacuum case*, *Class. Quant. Grav.* **13** (1996) 1241 [gr-qc/9505036] [INSPIRE].

[6] J.-H. Chen and Y.-J. Wang, *Chaos around charged black hole with dipoles*, gr-qc/0212092 [INSPIRE].



JHEP10(2023)189

[7] D.N. Page, D. Kubiznak, M. Vasudevan and P. Krtous, *Complete integrability of geodesic motion in general Kerr-NUT-AdS spacetimes*, *Phys. Rev. Lett.* **98** (2007) 061102 [hep-th/0611083] [INSPIRE].

[8] W. Hanan and E. Radu, *Chaotic motion in multi-black hole spacetimes and holographic screens*, *Mod. Phys. Lett. A* **22** (2007) 399 [gr-qc/0610119] [INSPIRE].

[9] S. Chen, M. Wang and J. Jing, *Chaotic motion of particles in the accelerating and rotating black holes spacetime*, *JHEP* **09** (2016) 082 [arXiv:1604.02785] [INSPIRE].

[10] Y. Chervonyi and O. Lunin, *(Non)-integrability of geodesics in D-brane backgrounds*, *JHEP* **02** (2014) 061 [arXiv:1311.1521] [INSPIRE].

[11] S. Dalui, B.R. Majhi and P. Mishra, *Presence of horizon makes particle motion chaotic*, *Phys. Lett. B* **788** (2019) 486 [arXiv:1803.06527] [INSPIRE].

[12] K. Hashimoto and N. Tanahashi, *Universality in chaos of particle motion near black hole horizon*, *Phys. Rev. D* **95** (2017) 024007 [arXiv:1610.06070] [INSPIRE].

[13] S. Dalui, B.R. Majhi and P. Mishra, *Horizon induces instability locally and creates quantum thermality*, *Phys. Rev. D* **102** (2020) 044006 [arXiv:1910.07989] [INSPIRE].

[14] P. Basu and L.A. Pando Zayas, *Chaos rules out integrability of strings on $AdS_5 \times T^{1,1}$*, *Phys. Lett. B* **700** (2011) 243 [arXiv:1103.4107] [INSPIRE].

[15] P. Basu, P. Chaturvedi and P. Samantray, *Chaotic dynamics of strings in charged black hole backgrounds*, *Phys. Rev. D* **95** (2017) 066014 [arXiv:1607.04466] [INSPIRE].

[16] A.V. Frolov and A.L. Larsen, *Chaotic scattering and capture of strings by black hole*, *Class. Quant. Grav.* **16** (1999) 3717 [gr-qc/9908039] [INSPIRE].

[17] P. Basu and L.A. Pando Zayas, *Analytic non-integrability in string theory*, *Phys. Rev. D* **84** (2011) 046006 [arXiv:1105.2540] [INSPIRE].

[18] P. Basu, D. Das, A. Ghosh and L.A. Pando Zayas, *Chaos around holographic Regge trajectories*, *JHEP* **05** (2012) 077 [arXiv:1201.5634] [INSPIRE].

[19] P. Basu and L.A. Pando Zayas, *Analytic non-integrability in string theory*, *Phys. Rev. D* **84** (2011) 046006 [arXiv:1105.2540] [INSPIRE].

[20] L.A. Pando Zayas and C.A. Terrero-Escalante, *Chaos in the gauge/gravity correspondence*, *JHEP* **09** (2010) 094 [arXiv:1007.0277] [INSPIRE].

[21] P. Basu, D. Das and A. Ghosh, *Integrability lost*, *Phys. Lett. B* **699** (2011) 388 [arXiv:1103.4101] [INSPIRE].

[22] N. Beisert et al., *Review of AdS/CFT integrability: an overview*, *Lett. Math. Phys.* **99** (2012) 3 [arXiv:1012.3982] [INSPIRE].

[23] S.J. van Tongeren, *Integrability of the $AdS_5 \times S^5$ superstring and its deformations*, *J. Phys. A* **47** (2014) 433001 [arXiv:1310.4854] [INSPIRE].

[24] R. Ricci, A.A. Tseytlin and M. Wolf, *On T-duality and integrability for strings on AdS backgrounds*, *JHEP* **12** (2007) 082 [arXiv:0711.0707] [INSPIRE].

[25] I. Bena, J. Polchinski and R. Roiban, *Hidden symmetries of the $AdS_5 \times S^5$ superstring*, *Phys. Rev. D* **69** (2004) 046002 [hep-th/0305116] [INSPIRE].

[26] K.S. Rigatos, *Nonintegrability of $L^{a,b,c}$ quiver gauge theories*, *Phys. Rev. D* **102** (2020) 106022 [arXiv:2009.11878] [INSPIRE].



JHEP10(2023)189

[27] T. Ishii, K. Murata and K. Yoshida, *Fate of chaotic strings in a confining geometry*, *Phys. Rev. D* **95** (2017) 066019 [arXiv:1610.05833] [INSPIRE].

[28] Y. Asano, D. Kawai, H. Kyono and K. Yoshida, *Chaotic strings in a near Penrose limit of $AdS_5 \times T^{1,1}$*, *JHEP* **08** (2015) 060 [arXiv:1505.07583] [INSPIRE].

[29] K. Hashimoto, K. Murata and N. Tanahashi, *Chaos of Wilson loop from string motion near black hole horizon*, *Phys. Rev. D* **98** (2018) 086007 [arXiv:1803.06756] [INSPIRE].

[30] C. Nunez, D. Roychowdhury and D.C. Thompson, *Integrability and non-integrability in $N = 2$ SCFTs and their holographic backgrounds*, *JHEP* **07** (2018) 044 [arXiv:1804.08621] [INSPIRE].

[31] D. Roychowdhury, *Analytic integrability for strings on $\eta$ and $\lambda$ deformed backgrounds*, *JHEP* **10** (2017) 056 [arXiv:1707.07172] [INSPIRE].

[32] A. Banerjee and A. Bhattacharyya, *Probing analytical and numerical integrability: the curious case of $(AdS_5 \times S^5)_\eta$*, *JHEP* **11** (2018) 124 [arXiv:1806.10924] [INSPIRE].

[33] D.-Z. Ma, J.-P. Wu and J. Zhang, *Chaos from the ring string in a Gauss-Bonnet black hole in $AdS_5$ space*, *Phys. Rev. D* **89** (2014) 086011 [arXiv:1405.3563] [INSPIRE].

[34] D. Giataganas and K. Sfetsos, *Non-integrability in non-relativistic theories*, *JHEP* **06** (2014) 018 [arXiv:1403.2703] [INSPIRE].

[35] A. Stepanchuk and A.A. Tseytlin, *On (non)integrability of classical strings in p-brane backgrounds*, *J. Phys. A* **46** (2013) 125401 [arXiv:1211.3727] [INSPIRE].

[36] D. Giataganas and K. Zoubos, *Non-integrability and chaos with unquenched flavor*, *JHEP* **10** (2017) 042 [arXiv:1707.04033] [INSPIRE].

[37] Y. Sekino and L. Susskind, *Fast scramblers*, *JHEP* **10** (2008) 065 [arXiv:0808.2096] [INSPIRE].

[38] J. Maldacena, S.H. Shenker and D. Stanford, *A bound on chaos*, *JHEP* **08** (2016) 106 [arXiv:1503.01409] [INSPIRE].

[39] S. Sachdev and J. Ye, *Gapless spin fluid ground state in a random, quantum Heisenberg magnet*, *Phys. Rev. Lett.* **70** (1993) 3339 [cond-mat/9212030] [INSPIRE].

[40] E. Marcus and S. Vandoren, *A new class of SYK-like models with maximal chaos*, *JHEP* **01** (2019) 166 [arXiv:1808.01190] [INSPIRE].

[41] A. Kitaev, *A simple model of quantum holography (part 1)*, in *Entanglement in strongly-correlated quantum matter*, https://online.kitp.ucsb.edu/online/entangled15/kitaev/, KITP, University of California, Santa Barbara, CA, U.S.A., 7 April 2015.

[42] A. Kitaev, *A simple model of quantum holography (part 2)*, in *Entanglement in strongly-correlated quantum matter*, https://online.kitp.ucsb.edu/online/entangled15/kitaev2/, KITP, University of California, Santa Barbara, CA, U.S.A., 27 May 2015.

[43] M. Čubrović, *The bound on chaos for closed strings in anti-de Sitter black hole backgrounds*, *JHEP* **12** (2019) 150 [arXiv:1904.06295] [INSPIRE].

[44] C. Gao, D. Chen, C. Yu and P. Wang, *Chaos bound and its violation in charged Kiselev black hole*, *Phys. Lett. B* **833** (2022) 137343 [arXiv:2204.07983] [INSPIRE].



JHEP10(2023)189

[45] B. Gwak, N. Kan, B.-H. Lee and H. Lee, *Violation of bound on chaos for charged probe in Kerr-Newman-AdS black hole*, *JHEP* **09** (2022) 026 [arXiv:2203.07298] [INSPIRE].

[46] N. Kan and B. Gwak, *Bound on the Lyapunov exponent in Kerr-Newman black holes via a charged particle*, *Phys. Rev. D* **105** (2022) 026006 [arXiv:2109.07341] [INSPIRE].

[47] Y.-Q. Lei and X.-H. Ge, *Circular motion of charged particles near a charged black hole*, *Phys. Rev. D* **105** (2022) 084011 [arXiv:2111.06089] [INSPIRE].

[48] S. Dalui, B.R. Majhi and P. Mishra, *Presence of horizon makes particle motion chaotic*, *Phys. Lett. B* **788** (2019) 486 [arXiv:1803.06527] [INSPIRE].

[49] K. Hashimoto, K. Murata, N. Tanahashi and R. Watanabe, *Bound on energy dependence of chaos*, *Phys. Rev. D* **106** (2022) 126010 [arXiv:2112.11163] [INSPIRE].

[50] G.T. Horowitz and A. Strominger, *Black strings and P-branes*, *Nucl. Phys. B* **360** (1991) 197 [INSPIRE].

[51] K. Becker, M. Becker and J.H. Schwarz, *String theory and M-theory: a modern introduction*, Cambridge University Press, Cambridge, U.K. (2006) [DOI:10.1017/cbo9780511816086].

[52] I.R. Klebanov and A.A. Tseytlin, *Entropy of near extremal black p-branes*, *Nucl. Phys. B* **475** (1996) 164 [hep-th/9604089] [INSPIRE].

[53] K.-I. Ohshima, *Comments on the entropy and the temperature of non-extremal black p-brane*, hep-th/0508100 [INSPIRE].

[54] M.J. Duff, H. Lu and C.N. Pope, *The black branes of M theory*, *Phys. Lett. B* **382** (1996) 73 [hep-th/9604052] [INSPIRE].

[55] K.C.M. Cheung and R. Leung, *Wrapped NS5-branes, consistent truncations and Inönü-Wigner contractions*, *JHEP* **09** (2021) 052 [arXiv:2106.11318] [INSPIRE].

[56] G. Möller, S. Ouvry and S. Matveenko, *Dimensional reduction on a sphere*, *Int. J. Mod. Phys. B* **20** (2006) 3533.

[57] D.-Z. Ma, D. Zhang, G. Fu and J.-P. Wu, *Chaotic dynamics of string around charged black brane with hyperscaling violation*, *JHEP* **01** (2020) 103 [arXiv:1911.09913] [INSPIRE].

[58] X. Wu, T.-Y. Huang and H. Zhang, *Lyapunov indices with two nearby trajectories in a curved spacetime*, *Phys. Rev. D* **74** (2006) 083001 [arXiv:1006.5251] [INSPIRE].

[59] C. Froeschlé, E. Lega and R. Gonczi, *Fast Lyapunov indicators. Application to asteroidal motion*, *Celest. Mech. Dyn. Astron.* **67** (1997) 41.

[60] C. Froeschlé and E. Lega, *On the structure of symplectic mappings. The fast Lyapunov indicator: a very sensitive tool*, *Celest. Mech. Dyn. Astron.* **78** (2000) 167.

[61] D.-Z. Ma, Z.-C. Long and Y. Zhu, *Application of indicators for chaos in chaotic circuit systems*, *Int. J. Bifurcation Chaos* **26** (2016) 1650182.

[62] X. Wu and T.-Y. Huang, *Computation of Lyapunov exponents in general relativity*, *Phys. Lett. A* **313** (2003) 77 [gr-qc/0302118] [INSPIRE].

[63] J.J.M. Ruiz, *Differential Galois theory and non-integrability of Hamiltonian systems*, Springer, Basel, Switzerland (1999) [DOI:10.1007/978-3-0348-0723-4].

[64] J.J. Morales-Ruiz, J.-P. Ramis and C. Simó, *Integrability of Hamiltonian systems and differential Galois groups of higher variational equations*, *Annales Sci. Ecole Norm. Sup.* **40** (2007) 845.



JHEP10(2023)189

[65] L. Susskind, *Why do things fall?*, arXiv:1802.01198 [INSPIRE].

[66] H.L. Prihadi, F.P. Zen, D. Dwiputra and S. Ariwahjoedi, *Chaos and fast scrambling delays of a dyonic Kerr-Sen-AdS$_4$ black hole and its ultraspinning version*, *Phys. Rev. D* **107** (2023) 124053 [arXiv:2304.08751] [INSPIRE].

[67] Y.-G. Miao and N. Ohta, *Complete intersecting nonextreme p-branes*, *Phys. Lett. B* **594** (2004) 218 [hep-th/0404082] [INSPIRE].

JHEP10(2023)189